Marine Micropaleontology 127 (2016) 50–62

Contents lists available at ScienceDirect

Marine Micropaleontology

journal homepage: www.elsevier.com/locate/marmicro

Plankton biochronology for the last 772,000 years from the western South Atlantic Ocean

Felipe A.L. Toledo [a], Juliana P. Quadros [a,*], Edmundo Camillo Jr. [a], Ana Cláudia A. Santarosa [a], José-Abel Flores [b], Karen B. Costa [a]

[a] South Atlantic Paleoceanography Laboratory, Oceanographic Institute, University of Sao Paulo, 05508-120 Sao Paulo, Brazil
[b] Departamento de Geologia, Universidad de Salamanca, 37008 Salamanca, Spain

ARTICLE INFO

Article history:
Received 27 July 2015
Received in revised form 27 June 2016
Accepted 6 July 2016
Available online 7 July 2016

Keywords:
Calcareous plankton
Calcareous nannofossil
Planktonic foraminifera
Western South Atlantic
Biochronology

ABSTRACT

Calcareous microfossils have potential in the biostratigraphy of Pleistocene sediments and a clear relationship with paleoceanographic studies. Conversely, there are few quantitative biostratigraphic studies of chronologically-tuned events or sections in the western South Atlantic. In order to improve the stratigraphical framework for South Atlantic paleoceanographic studies, the present work attempts to review the last 772,000 years by carrying out a quantitative analysis of the calcareous nannofossil and planktonic foraminiferal assemblages by comparing them with a high resolution marine isotopic record ($\delta^{18}O$). This work is based on the analysis of two piston cores obtained from the continental slope of the Santos Basin in the Santos Drift, southeastern Brazilian Continental Margin. Twelve Pleistocene calcareous nannofossil events and twenty planktonic foraminifera events calibrated with oxygen isotopes and correlated with literature stratigraphies are discussed. This is the first calcareous plankton biochronology study for the last 772 kyr in the western South Atlantic Ocean. More studies in this region will help to establish a more precise biochronology for these calcareous microfossils. This study also presents six new biostratigraphic events of isotopically-caibrated planktonic foraminifera which can be used as markers in the western South Atlantic.

1. Introduction

Biochronological studies are scarce in sections from the South Atlantic, a water body that plays an important role in climatic and oceanic evolution (Wefer et al., 1996) and is crucial to understand global dynamics. Improved isotopic data has permitted the calibration of microfossil data (Raffi et al., 2006; Wade et al., 2011), allowing more accurate correlations between different locations, and consequently, the dating of biostratigraphic events. Over the last few decades, calcareous microfossils have shown potential use in the biostratigraphy of Pleistocene sediments and a clear relationship with paleoceanographic studies. Some examples of biochronological data include Gartner (1977), Thierstein et al. (1977), Matsuoka and Okada (1990), Raffi et al. (1993, 2006), Wei (1993), Hine and Weaver (1998), Bollmann et al. (1998), Flores and Marino (2002) and Golovina et al. (2008) for calcareous nannofossils and Aksu and Kaminski (1989), Martin et al. (1990, 1993), Jorissen et al. (1993), Martinez et al. (2007) and Wade et al. (2011) for planktonic foraminifera.

Conversely, there are few quantitative biostratigraphic studies of chronologically-tuned events or sections in the southwestern Atlantic (Vicalvi, 1999; Tokutake and Toledo, 2007; Pivel et al., 2013; Camillo et al., 2015). Unfortunately, they are time restricted, covering a maximum of 130,000 years B.P. For this reason, it is common to find local workers referring to biozone boundary ages previously defined from different localities, such as the Gulf of Mexico, Caribbean Sea and Tropical Atlantic (see Vicalvi, 1997; Antunes, 1994, 2007; Portilho-Ramos et al., 2006; Ferreira et al., 2012). Precise age determination and evaluation of the synchrony of micropaleontological data are essential for making age-control points, which then help to estimate ages and sedimentation rates or to interpret isotope, carbonate and magneto-stratigraphy records.

In order to improve the stratigraphical framework for South Atlantic paleoceanographic studies, the present work attempts to review the last 772,000 years by carrying out a quantitative analysis of the calcareous nannofossil and planktonic foraminiferal assemblages and by comparing them with a high-resolution marine isotopic record ($\delta^{18}O$).

2. Material and methods

2.1. Core locations

This work is based on the analysis of two piston cores,GL-854 - 25° 12′S, 42°37′ W, 2220 m depth and GL-852 - 25°01′S, 43°33′W, 1938 m

* Corresponding author.
E-mail address: jupq@usp.br (J.P. Quadros).

http://dx.doi.org/10.1016/j.marmicro.2016.07.002
0377-8398/

depth, obtained from the continental slope of the Santos Basin in the Santos Drift, southeastern Brazilian Continental Margin during the Fugro Explorer Campaign 2007 (Fig. 1).

The Santos Basin is a large sedimentary basin that has been the focus of attention in the oil industry over the past 30 years. Despite several earlier studies and the economic interest owing to its potential hydrocarbon reserves, its paleoceanographic evolution remains poorly known. The continuity of oil-industry investigations has resulted in a growing knowledge of the basin, involving both tectono-structural approaches (Chang and Kowsmann, 1987; Macedo, 1989, 1990; Chang et al., 1992; Demercian et al., 1993; Mohriak et al., 1995; Cobbold et al., 2001; Meisling et al., 2001) and sedimentary–stratigraphic approaches (Pereira and Macedo, 1990; Pereira, 1994; Modica and Brush, 2004).

The ocean surface dynamics is controlled by the South Atlantic subtropical gyre. Present day surface hydrography is dominated by the presence of the southward-flowing warm, saline and nutrient-depleted Brazil Current (BC) (Stramma and England, 1999; Rodrigues et al., 2007). The BC flows along the Brazilian margin to the Subtropical Convergence Zone where, around 38°S, it meets the Falkland Current. Seismic studies in the Santos Basin suggest that sedimentation from the Neogene to Recent times was dominated by surface oceanic circulation redistributing the sediments transferred to the basin during both relative sea-level high stands and low stands (Duarte and Viana, 2007).

2.2. Lithology

The core description was performed at a 1:20 scale and included color (GSA Color Chart), visual grain size, lithology and primary structures. Facies classification was based on the combination of grain size and $CaCO_3$ content, the latter being estimated by the intensity of the reaction with a 10% HCl solution, frequently calibrated by calcimetric analysis. Thus, a fine-grained facies is classified as a marl when the $CaCO_3$ content reaches between 60 and 30%, carbonate-rich mud between 30 and 18%, carbonate-poor mud between 18 and 5% and mud with a $CaCO_3$ content of <5%.

2.2.1. Core GL-854

Core GL-854 had a recovery of 2038 cm of a continuous record with no observed hiatuses, composed of carbonate-rich mud intercalated with carbonate-poor mud and marl. A total of 409 samples were studied for both micropaleontological and geochemical studies; each sample was 2 cm thick and taken at 5 cm intervals throughout the core. According to the adopted age model the sample interval results in a temporal resolution of approximately one sample every 2 kyr.

2.2.2. Core GL-852

Core GL-852 also provided a continuous record with no observed hiatuses and had a recovery of 2030 cm, composed of carbonate-poor mud intercalated with carbonate-poor mud and marl. This core was sampled for both micropaleontological and geochemical studies at 10 cm intervals between the core top and 1040 cm and 5 cm intervals from 1045 cm to the base of the core (2030 cm). GL-852 has 302 studied samples resulting in a temporal resolution of approximately one sample every 0.5–1 kyr.

2.3. Calcareous nannofossil and planktonic foraminifera preparations

Quantitative analyses of calcareous nannofossils and planktonic foraminifera of cores GL-854 and GL-852 were performed using relative abundances (%) of selected species for both biostratigraphic analyses in order to compare our data with those previously published.

For calcareous nannofossil slide preparations we followed the modified pipette strew slide technique (Antunes, 1997), whereby a small amount (0.2 g) of sediment is selected, placed in a vial with a constant volume of distilled water, stirred and then left to disintegrate for a few hours. After stirring again, a small amount of the suspension is pipetted onto a coverslip, dried on a hotplate, and then the coverslip is affixed to a labeled glass slide using Canada balsam. Slides were examined using a Zeiss Axio Image 2 optical microscope under cross-polarized light, at 1600× magnification. The taxonomic frameworks of Perch-Nielsen (1989); Bown (1998 and references therein) and Antunes (2007) have been followed for identification. For quantitative analysis, at least 300 nannoliths were counted per slide in a random number of fields of view. This allows a 95% level of confidence to be reached for all species present in at least 1% abundance (Patterson and Fishbein, 1989). Then, a second counting was employed to remove noise due to particularly abundant species (small placoliths <3 μm).

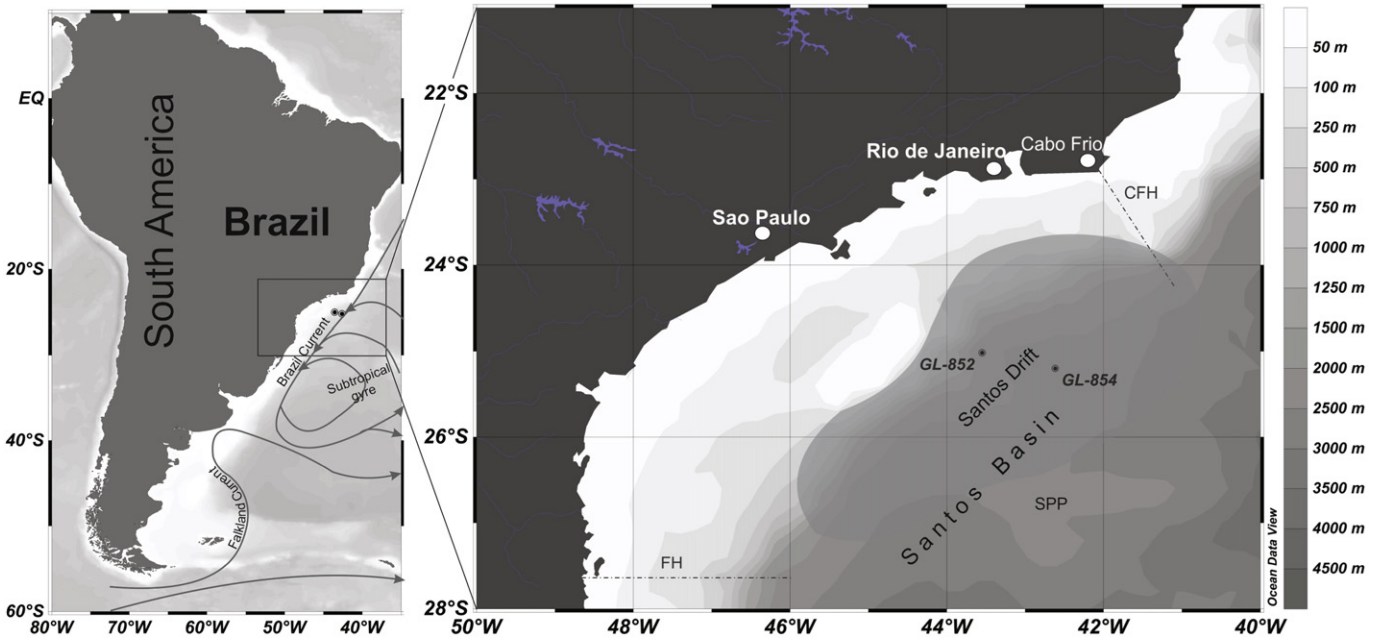

Fig. 1. Core locations and schematic figure of the oceanography and physiography of the study area. Arrows indicate surface flows and the shaded area the location of the Santos Drift. Dashed lines delimit the Santos Basin. FH: Florianopolis High; CFH: Cabo Frio High; SPP: Sao Paulo Plateau.

Table 1
Radiocarbon dating and respective calendar ages for core GL-854.

Core	Sample depth (cm)	^{14}C age	Error (^{14}C yr)	Reservoir effect (yr)	Calendar age (yr BP)	Error (1σ) (calendar age)
GL-854	0	3982	35	268	4442	40
	14	20,032	130	268	23,931	164
	51	37,832	250	268	42,850	275

Samples for planktonic foraminifera analyses were dry-sieved to make a 150 μm fraction and then split into subsamples containing at least 300 specimens of foraminifera (95% level of confidence for species of 1% abundance, Patterson and Fishbein, 1989). These subsamples were stored in micropaleontological slides, identified and counted. Identification follows the taxonomic criteria of Bolli and Saunders (1985) and Hemleben et al. (1989).

2.4. Preservation

Both microfossil groups were abundant throughout the cores. We simply recorded the general preservation state as excellent, good, moderate or poor. Calcareous nannofossil and planktonic foraminifera showed moderate to excellent preservation even during low carbonate content intervals. Carbonate stratigraphy for both cores correspond to the Atlantic-type, where higher carbonate content values correspond to interglacial intervals and lower carbonate content values occur during glacial intervals.

2.5. Stable isotope record and radiocarbon dating

One or two specimens of the benthic foraminifera *Cibicidoides wuellerstorfi* were selected from the >150 μm fraction and analyzed for their oxygen and carbon isotopic ratios. Stable isotope measurements were made at the *Scientific and Technological Centers of the University of Barcelona (CCiT-UB)* on a Finnigan MAT252 mass spectrometer with an integrated automated carbonate device and calibrated to Vienna Pee Dee Belemnite (VPDB) following standard procedures. During the course of this laboratory analysis, the external precision of the laboratory standards was $\delta^{18}O = 0.09\%$.

In core GL-854 three radiocarbon datings, in planktonic foraminifera *Globigerinoides ruber* 'white', were performed at the *National Ocean Science Accelerator Mass Spectrometrer Facility (NOSAMS)* at *Woods Hole Oceanographic Institution-WHOI*. The radiocarbon ages were transformed into calendar ages by first subtracting an estimated reservoir age of 268 years according to Butzin et al. (2005) using the program available at http://radiocarbon.LDEO.columbia.edu/and by applying the Fairbanks et al. (2005) calibration curve (version Fairbanks0107) (Table 1).

2.6. Biostratigraphic data

Four well established biostratigraphic events supported the chronological framework, they are: highest occurrence (HO) of *Pseudoemiliania lacunosa* (MIS 12), the lowest occurrence (LO) of *Emiliania huxleyi* (MIS 8), LO of *Globigerinella calida calida* (MIS 6) and the base of the *Globorotalia menardii* W Zone (MIS 6).

3. Age model

The age model (Fig. 2) was built based on the correlation of the benthic foraminifera oxygen isotope record and the Lisiecki and Raymo (2005) stack (LR04 reference curve) (Fig. 3) using the software Analyseries 2.0 (Paillard et al., 1996). Additionally, the three GL-854 ^{14}C AMS dates (Table 1) plus glacial terminations were used as control points in the model. Marine isotope stages are numbered according to Lisiecki and Raymo (2005) and Railsback et al. (2015). The marine isotope substages are lettered according to Railsback et al. (2015). The GL-854 age model is also presented in de Almeida et al. (2015).

The biochronological information from core GL-854 allows us to estimate a mean sedimentation rate of 4 cm/kyr. Minimum values (0.4 cm/kyr) were found at Terminations VII and VI, while the highest sedimentation rate is recorded during MIS 5 (up to 11 cm/kyr) (de Almeida et al., 2015). On the other hand, core GL-852 has a higher sedimentation rate, with mean values of ca. 7.4 cm/kyr. The minima values of 1 cm/kyr were recorded close to the MIS 9/MIS 8 and the highest values during MIS 5 (up to 25 cm/kyr). Core GL-854 extended to 772,000 yr before present (MIS 19 to MIS 1) (de Almeida et al., 2015) while core GL-852 covers the last 321,000 yr (MIS 9 to MIS 1) (Fig. 3).

4. Results and discussion

For both microfossil groups all the species presented in the assemblages were counted, but only species involved in the stratigraphic definition of events are considered in this study. Consequently, the relative abundances (%) presented in this study refer to the entire assemblage of calcareous nannofossils and/or planktonic foraminifera, rather than just the species with biostratigraphic significance. The category of 'small' *Gephyrocapsa* groups all the species of *Gephyrocapsa* < 3.5 μm (*Gephyrocapsa oceanica*, *Gephyrocapsa caribbeanica*, *Gephyrocapsa aperta*, *Gephyrocapsa ericsonii*, *Gephyrocapsa* c.f. *sinuosa* and *Gephyrocapsa* spp.). When showing the results regarding the *G.*

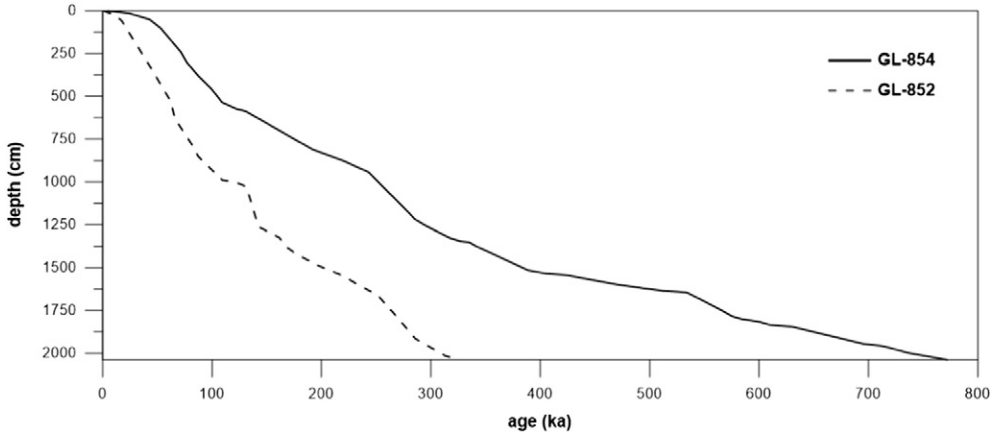

Fig. 2. Age-depth model for cores GL-854 and GL-852.

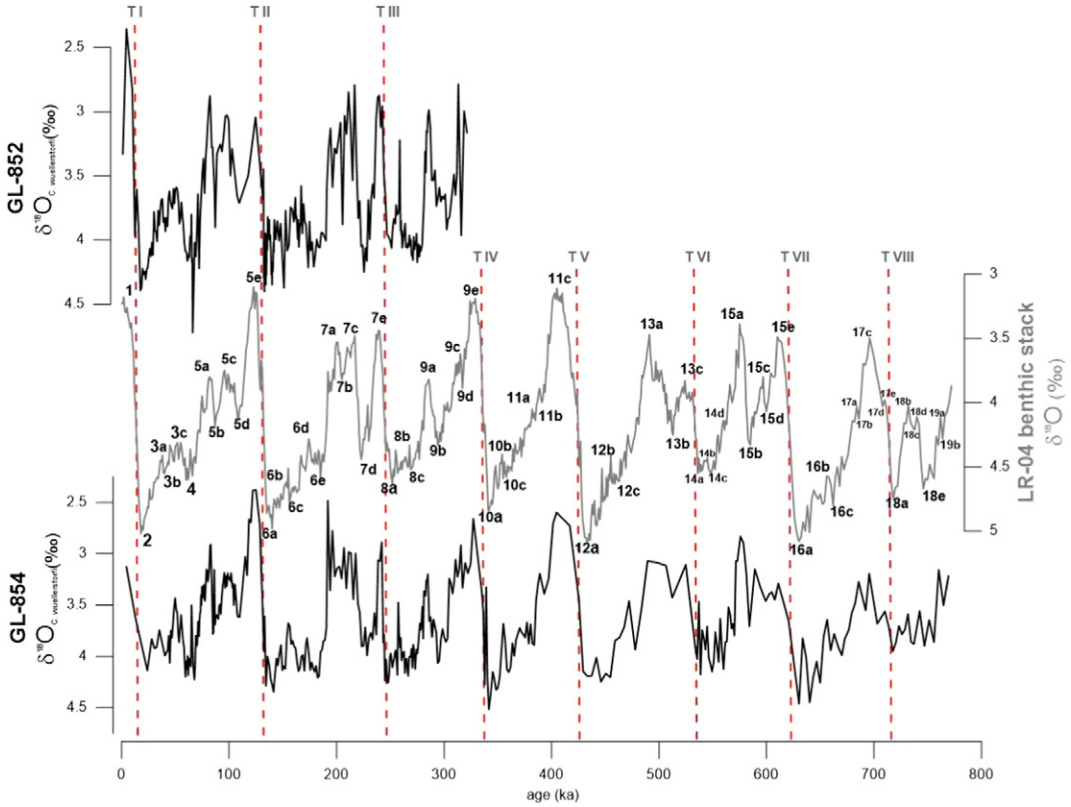

Fig. 3. Correlation between the GL-852 and GL-854 oxygen isotope signal and LR-04 benthic stack (Lisiecki and Raymo, 2005). Vertical red dotted lines indicate the glacial Terminations (T I to T VIII). Marine isotope stages are according to LR-04 stack and their substages are lettered according to Railsback et al. (2015). Analyseries linear correlation of 0.8 for both tuned age models.

aperta-ericsonii complex, we consider only the abundance of these two species together, since they have a similar interval of high abundance. The same could be observed for planktonic foraminifera categories of *G. menardii* complex and *G. crassaformis* complex (all subspecies of *G. menardii* and *G. crassaformis*). However, when the abundances of *Globorotalia tumida flexuosa*, *Globorotalia fimbriata*, *Globorotalia crassaformis imbricata* and *Globorotalia crassaformis hessi* are considered, their individual relative abundances, rather than those of the complexes are presented.

Correlations between events and isotope stages are proposed based on the adopted age model. The calcareous nannofossil zonation schemes proposed by Martini (1971) and Gartner (1977) were used as the basic zonal reference in this study, while that proposed by Antunes (2007) was used as a local zonal reference (Fig. 4A-C). The reference biozonation of Bolli and Saunders (1985) and Ericson and Wollin (1968) *G. menardii* biozones were employed for planktonic foraminifera (Fig. 5A-C).

The GL-854 sedimentary record begins during MIS 19 (at 772 ka) equivalent to calcareous nannofossil Zone NN 19 (Martini, 1971), *Pseudoemiliania lacunosa* Zone (Gartner, 1977) and interval D (Antunes, 2007). For planktonic foraminifera the GL-854 base is equivalent to the *G. crassaformis hessi* Subzone of the *Globorotalia truncatulinoides truncatulinoides* Zone (Bolli and Saunders, 1985). According to the Ericson and Wollin (1968) *G. menardii* biozones, our record begins inside the T Biozone (presence of *G. menardii* complex). The *G. menardii* complex exhibited three intervals of scarcity or absence, U, W and Y biozones, and three abundance intervals, V, X and Z biozones, during the last 772 kyr.

Used extensively in paleoclimate studies since the pioneering work of Ericson and Wollin (1968), these events are still drawing the attention of specialists today (Berger and Wefer, 1996; Sexton and Norris, 2011; Caley et al., 2012; Broecker and Pena, 2014). Here, the virtual disappearance of the *G. menardii* complex is marked when its relative abundance drops to 1% and the absence events were numbered top-down, D1, D2 and D3 (base of Y, W and U biozones, respectively) and reappearances as R1, R2 and R3 (base of Z, X and V biozones, respectively) (Fig. 5A-C).

4.1. Calcareous nannofossil events and biochronology (Figs. 4A-C)

4.1.1. Lowest occurrence (LO) of Helicosphaera inversa

The lowest occurrence of *H. inversa* in GL-854 was recorded just before the highest peak of MIS 18 (720.5 ka, 0.08% of abundance) (Table 2). This is the first record for the South Atlantic. This event has recently been re-evaluated by Maiorano et al. (2013) who highlighted great diachrony of the taxon between low and mid-latitudes records. According to these authors *H. inversa* first occurred at lower latitudes in the Pacific as early as 800 ka, while in the mid-latitude North Atlantic regions, it is not recorded before 510 ka. Our record is more recent than the Pacific but older than the North Atlantic record. Our record is in agreement with the Maiorano et al. (2013) hypothesis on the evolution of *H. inversa* in the Pacific during MIS 19 and a subsequent migration into the Atlantic as a cause of some of the observed distribution pattern. In GL-854 this taxon showed a gradual increase until its peak (0.6–0.7%) at the beginning of MIS 15 (610.9 ka). This peak is followed by a temporary disappearance from MIS 15 – MIS 12 (584.2 to 454.7 ka) very similar to that interval reported by Marino et al. (2003) in the Pacific Ocean.

4.1.2. Lowest Common Occurrence (LCO) of G. caribbeanica.

The LCO (continuous record after a significant increase in abundance) of *G. caribbeanica* was traceable exactly to the highest peak of MIS 15, around 568 ka (GL-854) (Table 2). This event was identified at the depth where the species reached an abundance higher than 20%. Bollmann et al. (1998) reported a similar observation in two North

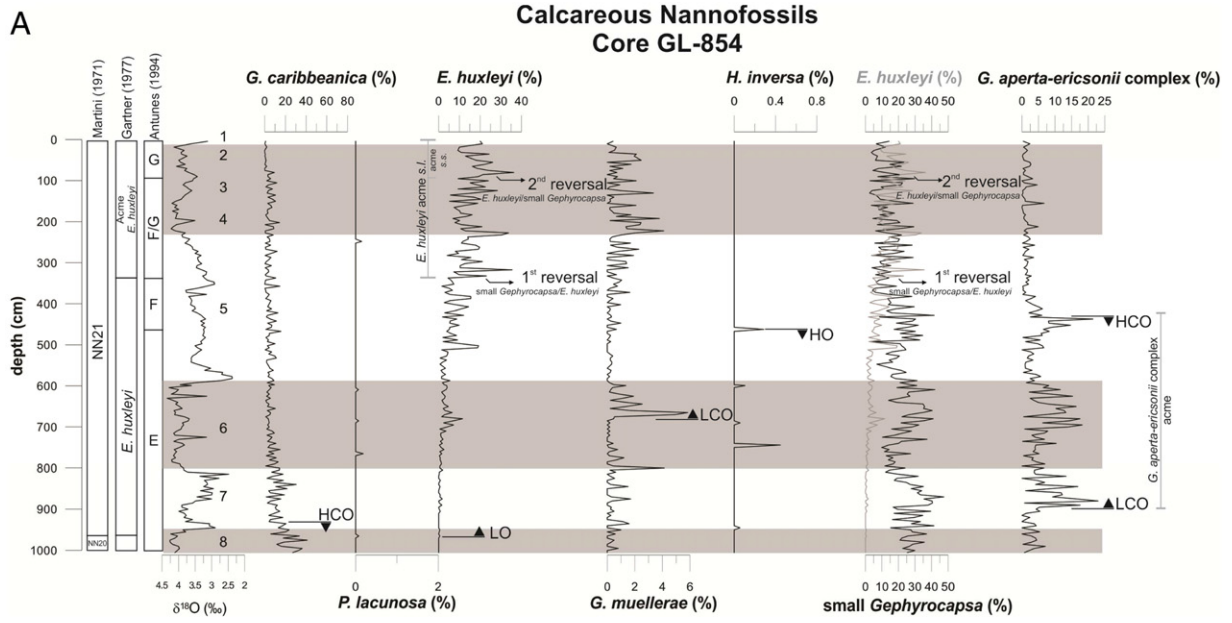
A
Calcareous Nannofossils
Core GL-854
G. caribbeanica (%)
E. huxleyi (%)
H. inversa (%)
E. huxleyi (%)
G. aperta-ericsonii complex (%)
Martini (1971)
Gartner (1977)
Antunes (1994)
depth (cm)
NN21
NN20
E. huxleyi
G. oceanica
Acme E. huxleyi
G
F/G
H
I
E. huxleyi acme s.l.
acme s.s.
2nd reversal
E. huxleyi/small Gephyrocapsa
1st reversal
small Gephyrocapsa/E. huxleyi
HO
LCO
HCO
LO
G. aperta-ericsonii complex acme
δ18O (‰)
P. lacunosa (%)
G. muellerae (%)
small Gephyrocapsa (%)

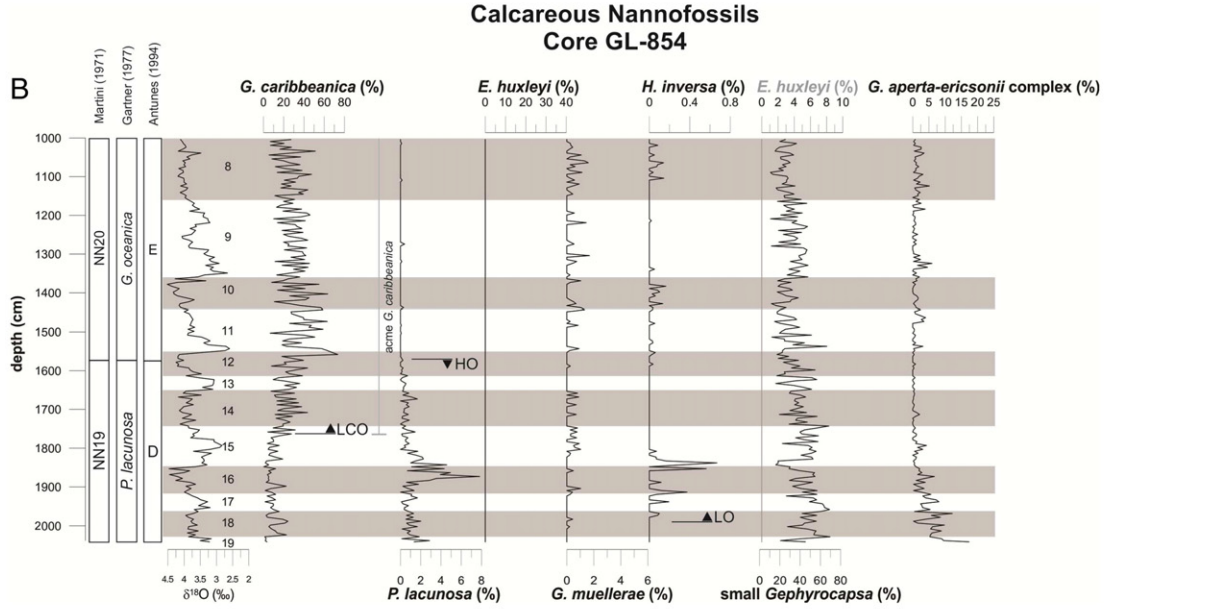
B
Calcareous Nannofossils
Core GL-854
G. caribbeanica (%)
E. huxleyi (%)
H. inversa (%)
E. huxleyi (%)
G. aperta-ericsonii complex (%)
Martini (1971)
Gartner (1977)
Antunes (1994)
depth (cm)
NN20
NN19
G. oceanica
P. lacunosa
m
D
acme G. caribbeanica
HO
LCO
LO
δ18O (‰)
P. lacunosa (%)
G. muellerae (%)
small Gephyrocapsa (%)

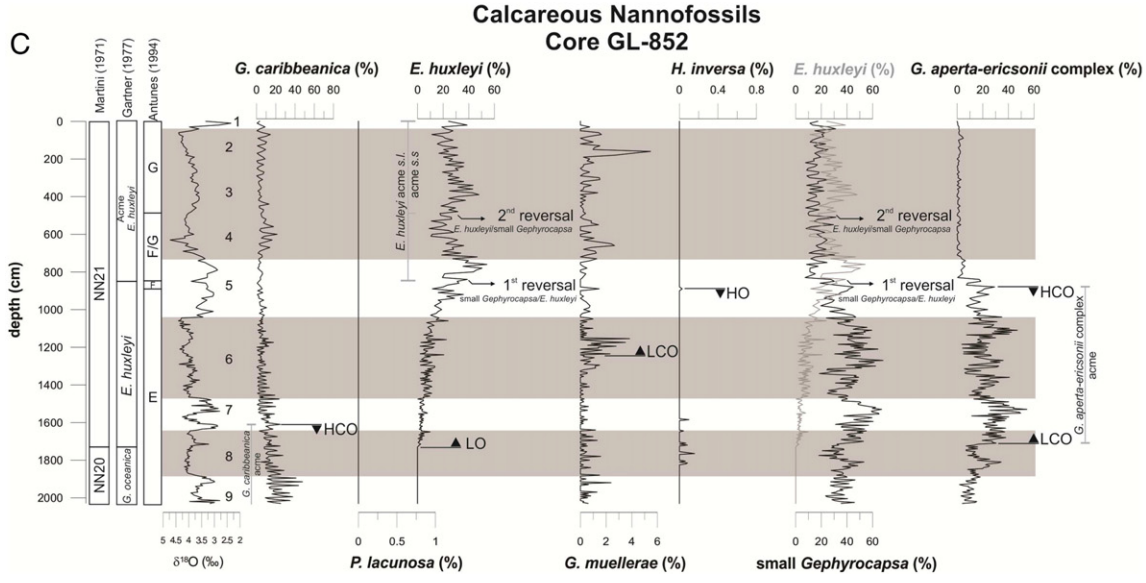
C
Calcareous Nannofossils
Core GL-852
G. caribbeanica (%)
E. huxleyi (%)
H. inversa (%)
E. huxleyi (%)
G. aperta-ericsonii complex (%)
Martini (1971)
Gartner (1977)
Antunes (1994)
depth (cm)
NN21
NN20
E. huxleyi
G. oceanica
Acme E. huxleyi
G
F/G
H
I
E. huxleyi acme s.l.
acme s.s
2nd reversal
E. huxleyi/small Gephyrocapsa
1st reversal
small Gephyrocapsa/E. huxleyi
HO
LCO
HCO
LO
G. caribbeanica acme
G. aperta-ericsonii complex acme
δ18O (‰)
P. lacunosa (%)
G. muellerae (%)
small Gephyrocapsa (%)

Atlantic deep sea cores (ODP 643 A and K708-7) as well as Flores et al. (2003) who identified the LCO of *G. caribbeanica* around 540 ka at Cape Basin (ODP Site 1089). Flores and Marino (2002) reported this event at the top of MIS 14 in the Southern Ocean; they have also called attention to the progressive increase of this species from MIS 15 prior to its dominance. Between MIS 12 and MIS 10 we observed a unique interval when *G. caribbeanica* exceeded 50% of the total assemblage in several samples. The highest abundance (73.5%) was recorded during Termination V, since then the trend has gradually reduced.

4.1.3. Highest occurrence (HO) of Pseudoemiliania lacunosa

The HO of *P. lacunosa* is a globally synchronous event, consistently occurring within MIS 12 (Thierstein et al., 1977; Hine, 1990; Raffi et al., 2006). In core GL-854 this event could be identified in the highest peak of MIS 12, at 433 ka (Table 2), with an abundance of 0.03%. The HO of *P. lacunosa* was reported at 440 ka in the Equatorial Atlantic (Raffi et al., 2006), 447 ka in Cape Basin (Flores et al., 2003) and 450 ka in the Southern Ocean (Flores and Marino, 2002). In the Equatorial Pacific this event was dated as 436 ka and in the Eastern Mediterranean as 465 ka (Raffi et al., 2006). In GL-854 a *P. lacunosa* peak (7.8%) was observed between MIS 16/MIS 15 (660 ka), similar to that *reported by Thierstein* et al. *(1977)*. *Pseudoemiliania lacunosa* abundance was higher than 2% of the total assemblage during a 70 kyr long interval (660 to 589 ka).

4.1.4. Lowest occurrence of E. huxleyi and highest common occurrence (HCO) of G. caribbeanica (acme zone)

The LO of *E. huxleyi* was dated by Thierstein et al. (1977) at 268 ka (MIS 8) as a synchronous event. This synchronism is corroborated by Raffi et al. (2006) who reported the age of 265 ka in the Eastern Mediterranean and 289 ka in the Equatorial Atlantic. In core GL-854, *E. huxleyi* was found for the first time at the highest peak of MIS 8, between MIS 8b and 8a dated as 246 ka (GL-854, 0.5%) and 259 ka (GL-852, 0.8%) (Table 2). According to Hine and Weaver (1998) it is a slightly time-transgressive event occurring in progressively younger sediments from north to south in the NE Atlantic. The HCO (dramatic reduction) of *G. caribbeanica* is an event close to the LO of *E. huxleyi*. Here, a clear reduction in the abundance of *G. caribbeanica* (<20%) occurs at the bottom of MIS 7, around 237 ka (GL-854) and 234 ka (GL-852) near the MIS 7e-7d transition. Our results and previous data agree with a global synchronism (Pujos and Giraudeau, 1993; Bollmann et al., 1998; Flores et al., 2000; Flores and Marino, 2002).

4.1.5. Lowest and highest common occurrence of G. aperta-ericsonii Complex (acme zone)

According to Hine and Weaver (1998), several acme events of the Noelaerhabdaceae preceded the widespread acme of *E. huxleyi*. These acme events are well known in North Atlantic sites (Hine and Weaver, 1998). In the Santos Basin we could recognize some of them and here we report one that is equivalent to the *G. aperta* Acme Zone (Hine and Weaver, 1998). In our analyses, we integrated *G. aperta* and *G. ericsonii* (*G. aperta-ericsonii* complex) to define this highlighted abundance (>10% of the total assemblage) interval because of their temporal correlation.

Three distinct peaks promptly characterized the *G. aperta-ericsonii* complex zone. During this interval, the relative abundance of the complex reached >20% in GL-854 and >40% in GL-852. In GL-854, the whole zone spans the middle of MIS 7, all MIS 6 and the lower part of MIS 5, which is similar to the acme of 'small' *Gephyrocapsa* reported by Pujos and Giraudeau (1993). The LCO of these species in GL-854 was traceable close to the MIS 7e peak and dated at 232 ka. At 84 ka was situated the HCO of *G. aperta-ericsonii* complex, close to the MIS 5c-5b transition. On the other hand, the LCO of *G. aperta-ericsonii* complex record in GL-852 was dated at 257.5 ka and their HCO at 84 ka (Table 2). This acme zone in core GL-852 is longer than that of GL-854, comprising the upper part of MIS 8 to the middle of MIS 5, which makes the LCO itself not so clear. The good preservation observed in GL-852 during this period enabled the identification of these very small species. Even with the uncertainty of the LCO, the timing of the HCO at 84 ka is remarkable. Further studies in this region should be carried out in order to verify the consistency of these events as biostratigraphic markers.

4.1.6. Lowest common occurrence of Gephyrocapsa muellerae.

The LCO of *G. muellerae* was registered around 152 ka in GL-854 and 141 ka in GL-852, at MIS 6b (Table 2). We consider those values higher than 2% of total assemblage to define *G. muellerae* 'common occurrence', since this species is not abundant in our records. This event has also been reported to occur in the Atlantic sector of the Southern Ocean around 150 ka (Flores and Marino, 2002). It also seems to be a global synchronous event as the HCO of *G. caribbeanica* (Pujos and Giraudeau, 1993; Flores et al., 1999, 2000, 2003). The two peaks of *G. muellerae* correspond to glacial intervals (MIS 6 and MIS 4–2).

4.1.7. Highest occurrence (HO) of H. inversa

The highest occurrences of *H. inversa* were recorded at 99.5 ka, substage 5c in core GL-854 (0.29%) and at 93.5 ka, between substages 5c and 5b, in core GL-852 (0.03%) (Table 2). Our record is younger than the average age of 150–140 kyr (MIS 6) of previous studies (Takayama and Sato, 1987; Hine, 1990), but Hine and Weaver (1998) reported that it is a slightly time-transgressive event (over 47 kyr). Because both sites give consistent ages for this event, we do not consider it to be a result of reworking during MIS 5.

4.1.8. E. huxleyi traditional acme and reversals in small Gephyrocapsa ssp – E. huxleyi

In our material, the base of the traditional *E. huxleyi* acme was registered at 80 ka, during substage 5a (GL-854, 23%), and at 73 ka, at the end of the substage 5a (GL-852, 33%), very close to the MIS 5/MIS 4 boundary (Table 2). Thierstein et al. (1977) showed this event to be diachronous between 85 ka in low latitudes and 73 ka in transitional waters, restricting this event to MIS 5. Hine (1990) recorded this event at dates as young as 62 ka in the North Atlantic, extending this event to MIS 4. Gartner (1977) dated the *E. huxleyi* acme base at 70 ka. Here, we consider the abrupt rise in the *E. huxleyi* record (20%) to define the base of this acme zone (which we call *E. huxleyi* acme sensu lato). This abrupt rise was observed just after the highest peak of MIS 5a. However, this *E. huxleyi* rise was not visually noticeable in the optical microscope, because of the very abundant small *Gephyrocapsa* spp. in the assemblage. This pattern is observed only when quantitative analyses are undertaken.

Flores et al. (2000) highlighted that differences from place-to-place in the proportion of *E. huxleyi* may cause confusion when employing terms such as "acme" or "zone of dominance". As pointed out by several authors (Thierstein et al., 1977; Jordan et al., 1996; Flores et al., 2000, 2003), the inherent diachronism of the *E. huxleyi* acme makes it difficult to recognize in cores from certain areas. For this reason, Thierstein et al. (1977) proposed the use of reversal in abundance of *G. caribbeanica – E. huxleyi* (*G. muellerae – E. huxleyi*) dated as 85–73 kyr, as a biostratigraphic event. Berggren et al. (1995) dated the same event as 75 ka. In our study area, we propose the reversal in abundance of small *Gephyrocapsa* spp. – *E. huxleyi*, where small *Gephyrocapsa* spp. refers

Fig. 4. A: Calcareous nannofossil events identified in GL-854 (0–1000 cm), oxygen isotope curve and reference zonal schemes. Gray bands correspond to marine isotopic stages. B: Calcareous nannofossil events identified in GL-854 (1000–2038 cm), oxygen isotope curve and reference zonal schemes. Gray bands correspond to marine isotopic stages. C: Calcareous nannofossil events identified in GL-852 (0–2030 cm), oxygen isotope curve and reference zonal schemes. Gray bands correspond to marine isotopic stages.

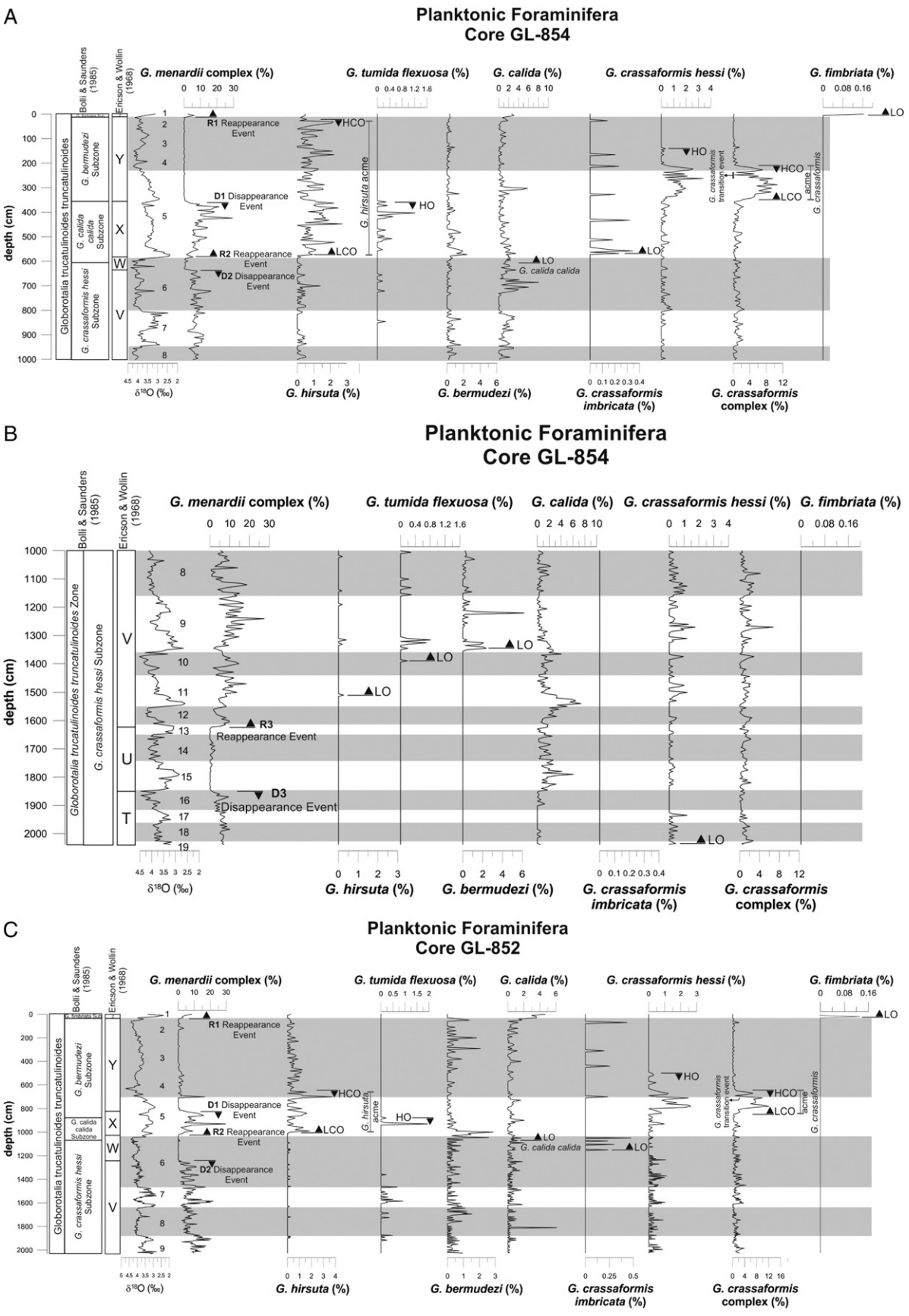

Fig. 5. A: Quaternary planktonic foraminifera events identified in GL-854 (0–1000 cm), oxygen isotope curve and reference zonal schemes. Gray bands correspond to marine isotopic stages. B: Quaternary planktonic foraminifera events identified in GL-854 (1000–2038 cm), oxygen isotope curve and reference zonal schemes. Gray bands correspond to marine isotopic stages. C: Quaternary planktonic foraminifera events identified in GL-852 (0–2030 cm), oxygen isotope curve and reference zonal schemes. Gray bands correspond to marine isotopic stages.

Table 2
Pleistocene calcareous nannofossil and planktonic foraminifera events and their calibrated ages in the studied cores.

Group	Events	Ages (kyr)			MIS	Age (kyr)	Local	References
		GL-854	GL-852	Mean				
calcareous nannofossils	LO *H. inversa*	720,5	x	720,5	18	800 510	Pacific Ocean North Atlantic Ocean	Maiorano et al. (2013)
	LCO *G. caribbeanica*	568	x	568	15	540	Cape Basin	Flores et al. (2003)
	HO *P. lacunosa*	433	x	433	12	436	Equatorial Pacific	Raffi et al. (2006)
						440	Equatorial Atlantic	Raffi et al. (2006)
						447	Cape Basin	Flores et al. (2003)
						450	Southern Ocean	Flores and Marino (2002)
	LO *E. huxleyi*	246	260	253	8	268		Thierstein et al. (1977)
						265	Eastern Mediterranean	Raffi et al. (2006)
	LCO *G. aperta-ericsonii* complex	232	258	245	7-8	MIS 7		Pujos & Giraudeau (1993)
	HCO *G. caribbeanica*	237	234	235,5	7	MIS 7	Southern Ocean	Flores and Marino (2002)
						249	Cape Basin	Flores et al. (2003)
	LCO *G. muellerae*	152	141	146,5	6	150	Southern Ocean	Flores and Marino (2002)
						165	Cape Basin	Flores et al. (2003)
	HO *H. inversa*	99,5	93,5	96,5	5	150	North Atlantic	Takayama and Sato 1987
						140	Ocean	Hine and Weaver (1998)
	HCO *G. aperta-ericsonii* complex	84	84	84	5	MIS 6	North Atlantic Ocean	Hine and Weaver (1998)
	Small *Gephyrocapsa - E. huxleyi* (1st reversal)	80	84	82	5	65	Cape Basin	Flores et al. (2003)
	E. huxleyi acme base (s.l.)	80	73	76,5	5	85-73		Thierstein et al. (1977)
						85	Cape Basin	Flores et al. (2003)
						62	North Atlantic Ocean	Hine (1990)
	E. huxleyi - small *Gephyrocapsa* (2nd reversal)	50	57	53,5	3	45	Cape Basin	Flores et al. (2003)
planktonic foraminifera	LO *G. crassaformis hessi*	772	x	772	19	750	Pacific Ocean	Chaproniere et al. (1994)/Berggren et al. (1995)
						4.5 Ma	North Atlantic Ocean	Bylinskaya (2005)
	G. menardii D3	634	x	634	16	620-525	Gulf of Mexico	Martin et al. (1993)
						610	Gulf of Mexico	Kohl et al. (2004)
	G. menardii R3	494	x	494	13	485	Gulf of Mexico	Kohl et al. (2004)
						MIS 13	Caribbean Sea	Martin et al. (1990)
						MIS 13	Caribbean Sea	Martinez et al. (2007)
	LO *G. hirsuta*	387	x	387	11	450	SW Atlantic	Pujol and Duprat (1983)
	LO *G. tumida flexuosa*	347	x	347	10	400		Berggren et al. (1995)
						400	Pacific Ocean	Wade et al. (2011)
	LO *G. bermudezi*	335	x	335	9			
	G. menardii D2	142,7	142	142,4	6	186	Gulf of Mexico	Kohl et al. (2004)
						200	Gulf of Mexico	Martin et al. (1993)
						MIS 6	Caribbean Sea	Martinez et al. (2007)
	LO *G. calida calida*	137	133,5	135,3	6	140	Equatorial Atlantic	Bolli and Premoli Silva (1973)
						220	Pacific Ocean	Chaproniere et al. (1994)
							Pacific Ocean	Wade et al. (2011)
	LO *G. crassaformis imbricata*	120,4	132,4	126,4	5	580	North Atlantic Ocean	Bylinskaya (2005)
	G. menardii R2	129	128,5	128,8	5	130	Gulf of Mexico	Kohl et al. (2004)
						127	Campos Basin	Vicalvi (1997)
	LCO *G. hirsuta*	122	118	120	5			This study
	HO *G. tumida flexuosa*	84	93,5	88,75	5			
	G. menardii D1	84	84	84	5	84	Campos Basin	Vicalvi (1997)
						89	Gulf of Mexico	Kohl et al. (2004)
						90	Gulf of Mexico	Martin et al. (1993)
	LCO *G. crassaformis* complex	82	83,9	82,95	5			This study
	G. crassaformis transition event	72	72	72	MIS 5/4			This study
	HCO *G. crassaformis* complex	68,5	69,1	68,8	4			This study
	HO *G. crassaformis hessi*	58,2	59,4	58,8	4	190	Tropical Atlantic	Bylinskaya (2005)
	HCO *G. hirsuta*	33	34	33,5	3			This study
	G. menardii R1	12	12	12	1	11	Campos Basin	Vicalvi (1997)
						11	Gulf of Mexico	Kohl et al. (2004)
	LO *G. fimbriata*	12	10	11	1	11	Equatorial Atlantic	Bolli and Premoli Silva (1973)

to all those smaller than 3.5 μm, given that *G. muellerae* does not make up a significant percentage of the total assemblage.

A clear decrease in small *Gephyrocapsa* spp. relative abundance could be observed around 86 ka (GL-854 (6.2%) and GL-852 (7.4%)) prior to the *E. huxleyi* abrupt rise (20% in our record) (base of *E. huxleyi* acme s.l.) (Fig. 4A, C). This event is equivalent to the top of the F interval according to Antunes (1994, 2007). From the FO of *E. huxleyi* to the decrease in small *Gephyrocapsa* spp., the average *E. huxleyi* abundance represented only 3.2% (GL-854) and 5.3% (GL-852), while small *Gephyrocapsa* spp. were 24% (GL-854) and 42.5% (GL-852) of the total assemblage in the MIS 5a peak. At 80 ka and 84 ka (GL-854 and GL-852, respectively) the first small *Gephyrocapsa* – *E. huxleyi* reversal (g/

e) could be observed. Following this reversal, a transitional interval was identified with no dominance of either *E. huxleyi* or small *Gephyrocapsa.* This interval was considered of biostratigraphic significance as also mentioned by Antunes (1994, 1997 and 2007) (among others, Tokutake and Toledo (2007); Maciel et al. (2012)) who designated it as the F/G Transition. The end of the transitional interval is marked by the second small *Gephyrocapsa* spp. – *E. huxleyi* reversal (*e*/g) (traceable very close to the highest peak of MIS 3) from when the *E. huxleyi* dominance became remarkable. In GL-854 this reversal was registered as 50 ka during MIS 3 (*E. huxleyi* 19%; small *Gephyrocapsa* spp. 7%). In GL-852 the same reversal is somewhat older, being dated as 57 ka at the boundary between MIS 4/MIS 3 (*E. huxleyi* 31%; small *Gephyrocapsa* spp. 10%). Therefore, the *E. huxleyi* acme itself begins from this point and continues to the present day (*E. huxleyi* acme sensu stricto) (Fig. 4A, C).

4.2. Planktonic foraminifera events and biochronology (Fig. 5A-C)

4.2.1. Lowest occurrence (LO) of G. crassaformis hessi

The LO of *G. crassaformis hessi* (0.43%) was recognized at the base of GL-854 in the highest recorded peak of MIS 19 (Table 2). It suggests that the *G. crassaformis hessi* first occurrence could be prior to 772 ka in Santos Basin and older than those estimates by Chaproniere et al. (1994) and Berggren et al. (1995). These authors reported the *G. crassaformis hessi* first appearance datum around 750 ka. Bylinskaya (2005) has studied a set of cores in the North Atlantic and dated this event as old as 4.5 Ma in the mid-Lower Pliocene.

4.2.2. G. menardii complex disappearance event (D3)

The lowest *G. menardii* virtual disappearance (≤1% of total assemblage) event observed in GL-854 (D3) was dated at 634 ka (Table 2), just before Termination VII, in the highest peak of MIS 16. This event is equivalent to the bottom of the Ericson and Wollin (1968) U zone. The GL-854 record seems to occur prior to the ages given in previous studies: 620–525 kyr (Martin et al., 1993) and 610 ka (Kohl et al., 2004) both in Gulf of Mexico, as well as the age reported by Ferreira et al. (2012) for the same basin in South Atlantic (610 ka). However, the latter authors reported the ages calculated by Kohl et al. (2004).

4.2.3. G. menardii complex reappearance event (R3).

The lowest *G. menardii* reappearance event (R3) (≥1%) in GL-854 was registered just after the highest peak of MIS 13 and dated at 494 ka (Table 2). This reappearance marks the bottom of V zone (Ericson and Wollin, 1968). The apparent diachronism reported for the D3 event could also be observed in the R3 event, which is slightly older than the V zone recorded by Kohn et al. (2004) in the Gulf of Mexico and Ferreira et al. (2012) in the Santos Basin (485 ka). Martin et al. (1990) and Martinez et al. (2007) reported this event within MIS 13 in the Caribbean Sea.

4.2.4. Lowest occurrences of Globorotalia hirsuta, G. tumida flexuosa and Globigerina bermudezi

Pujol and Duprat (1983) dated the lowest occurrence (LO) of *G. hirsuta* at 450 ka at the Rio Grande Rise (SW Atlantic), the same age was reported by Wade et al. (2011). In core GL-854 this event is younger and recorded by 0.27% *G. hirsuta* at 387 ka, a dip just before the highest peak of MIS 11. The LO of *G. tumida flexuosa* in GL-854 (0.19%) was identified in the MIS 10b-10a transition around 347 ka, while previous studies dated this event at 400 ka (Berggren et al., 1995; Wade et al., 2011). Very close to this event, early in MIS 9, we recognized the LO of *G. bermudezi* (0.38%), dated at 335 ka, shortly after Termination IV. The latter event is registered only in a table in Bolli and Saunders (1985), showing its first occurrence during the Subzone *G. crassaformis hessi*. Here we calibrated isotopically the LO in core GL-854 and estimate an age for this event (Table 2). In GL-852, these events were not recorded since the GL-852 base sample is younger than them.

4.2.5. G. menardii complex disappearance event (D2)

This virtual disappearance of the *G. menardii* complex (≤1%) was recorded at 142 ka during MIS 6b, with an abundance of 0.25% in GL-854 and of 0.36%in GL-852 (Table 2). The D2 disappearance event corresponds to the bottom of the Ericson and Wollin (1968) W zone. Martinez et al. (2007) found the same event during MIS 6, while Martin et al. (1990) recorded it at the MIS 7/MIS 6 boundary, both in the Caribbean Sea. Our records are subsequent to those reported by Martin et al. (1993) (200 ka, MIS 7), Kohl et al. (2004) (186 ka, MIS 6) in the Gulf of Mexico and Ferreira et al. (2012) (186 ka) in the Santos Basin.

4.2.6. Lowest occurrence of G. calida calida.

In GL-854 the LO of *G. calida calida* was observed around 137 ka and in GL-852 this event was marked at 133.5 ka (Table 2), somewhat before the highest peak of MIS 6, in the beginning of MIS 6a, within the *G. menardii* W zone. The LO of *G. calida calida* marks the base of the evolutionary *G. calida calida* Subzone. This event has been dated at 140 ka in the Equatorial Atlantic (Bolli and Premoli Silva, 1973) and 220 ka in the Pacific Ocean (Chaproniere et al., 1994; Wade et al., 2011).

4.2.7. Lowest occurrence (LO) of Globorotalia crassaformis imbricata (Krasheninnikov and Bylinskaya, 2002)

The LO of *G. crassaformis imbricata* was identified and dated at 120.4 ka (GL-854, 0.23%), during substage 5e, and at 132.4 ka (GL-852, 0.48%), near Termination II (Table 2). This event occurred in the lower half of the *G. calida calida* subzone as also noted by Bylinskaya (2005). However, this author dated the event at approximately 580 ka, before our records.

4.2.8. G. menardii complex reappearance event (R2)

The R2 virtual reappearance event of the *G. menardii* complex (≥1%) was recorded also very close to Termination II, dated at 129 ka (5%), in GL-854 and at 128.5 ka in GL-852 (3%) (Table 2). This reappearance event is equivalent to the bottom of the X zone (Ericson and Wollin, 1968) and seems to be synchronous (Vicalvi, 1997; Kohl et al., 2004; Martinez et al., 2007).

4.2.9. Lowest and highest common occurrences of G. hirsuta (acme zone) (this study)

We recognized the LCO of *G. hirsuta,* a continuous record after a significant increase in its abundance, near to the R2 *G. menardii* event. The LCO of *G. hirsuta* was registered around 122 ka (GL-854) by 0.93% and 118 ka(GL-852) by 1.84% at the MIS 5e-5d transition and the HCO was dated at 33 ka (GL-854) (2%) and 34 ka (GL-852) (0.92%) in the first dip before the highest peak of MIS 3 (Table 2). Although this species constitutes a small portion of the whole assemblage, the increase of >17 times its relative abundance is particularly evident. The mean *G. hirsuta* relative abundance was 0.72% between its LCO and HCO, against 0.04% out of this interval (GL-854 and GL-852 mean values). These events have never been reported from the Brazilian continental margin. This 84.5 kyr long (mean) interval can be recognized as an acme zone because of the LO of *G. hirsuta* as well as being an important biostratigraphical marker in the western South Atlantic.

4.2.10. G. menardii complex disappearance event (D1) and highest occurrence of G. tumida flexuosa

The D1 virtual disappearance event of the *G. menardii* complex (≤1%) was dated at 84 ka, during the oxygen isotopic substage 5b (Table 2) in both records (0.53% GL-854 and 0.47% GL-852). According to our results, and previous studies (Vicalvi, 1997; Portilho-Ramos et al., 2006; Ferreira et al., 2012), this event is synchronous and coincident with Ericson and Wollin (1968) X/Y boundary zones. In core GL-854 the D1 event also occurs at the base of the *G. bermudezi* Subzone (Bolli and Saunders, 1985), which is defined by the HO of *G. tumida flexuosa* (0.28%). However, in GL-852 the HO of *G. tumida flexuosa* (0.22%) was

registered 9.5 kyr prior to the GL-854 record, at 93.5 ka within X biozone (Ericson and Wollin, 1968). In GL-852 the base of the *G. bermudezi* Subzone (Bolli and Saunders, 1985) is located between substages 5c and 5b.

4.2.11. Lowest and highest common occurrences of G. crassaformis complex (acme zone) and G. crassaformis transition event (this study)

The LCO of the *G. crassaformis* complex occurred at 82 ka (GL-854, 4.3%) and 83.9 ka (GL-852, 4.9%), within substage 5b, when a sudden increase in this group's abundance was recognized just after the well-dated D1 event. This continuous record (mean abundance 6% in GL-854 and GL-852) extended up to what we called the HCO event of the *G. crassaformis* complex at 68.5 ka (GL-854, 4.3%) and 69.1 ka (GL-852, 3.6%) at the base of MIS 4 just before the highest peak of this MIS.

Our quantitative biostratigraphy allows us to observe an increase of >7 times the *G. crassaformis* complex relative abundance out of this interval from 0.86% to 6.4%, on average (GL-854 and GL-852). Some authors (Vicalvi, 1997; Toledo, 2000; Sanjinés, 2006; Camillo, 2007) have already mentioned such an increment in *G. crassaformis* along the Brazilian continental margin and recently, Portilho-Ramos et al. (2014) have reported the same feature, described as the *G. crassaformis* Optimum Event. This 14 kyr (on average) long interval can be recognized as an acme zone, as well as an important biostratigraphical marker in the western South Atlantic. On the other hand, Bylinskaya (2005) carried out a detailed study on the range and significance of the *G. crassaformis* complex in a set of cores in the North Atlantic, but did not describe such events or an acme zone.

It was also possible to recognize in our record a dramatic and punctual reduction between the LCO-HCO of the *G. crassaformis* complex interval (Fig. 5A, C). We could recognize this consistent drop in *G. crassaformis* complex abundance not only in our record but also in other studies (Vicalvi, 1997; Toledo, 2000; Sanjinés, 2006; Camillo, 2007; Portilho-Ramos et al., 2014). Therefore, this feature is a useful biostratigraphical marker due to its proximity to the MIS 5/MIS 4 transition. Particularly in core GL-854 and GL-852 it occurred at 72 ka (Table 2), but we calculated an average age of 71 ka for this feature for five cores along the Brazilian continental margin (*unpublished data*). Indeed, 71 ka is the MIS 5/MIS 4 boundary itself. We called this feature the *G. crassaformis* transition event.

4.2.12. Highest occurrence of G. crassaformis hessi

The HO of *G. crassaformis hessi* was recorded at the highest peak of MIS 4, close to the MIS4/MIS 3 transition, at 58.2 ka by 0.33% abundance (GL-854) and 59.4 ka by 0.20% abundance (GL-852). This event is placed between 100 and 200 ka by Bylinskaya (2005), who also observed it at 190 ka in the Tropical Atlantic (15°N).

4.2.13. G. menardii complex reappearance event (R1)

The highest *G. menardii* complex reappearance event (R1) (≥1%) was recorded at 12 ka already during MIS1 in cores GL-854 (6%) and GL-852 (3%) (Table 2). This event is equivalent to the Ericson and Wollin's (1968) Y/Z boundary zone. Some authors have dated this reappearance event at 11 ka (Vicalvi, 1997; Kohl et al., 2004).

4.2.14. Lowest occurrence of G. fimbriata

The LO of *G. menardii fimbriata* was registered at 12 ka in core GL-854 and at 10 ka in GL-852, both already during MIS 1 (Table 2). This event marks the *G. fimbriata* Subzone of Bolli and Saunders (1985).

4.3. Calcareous plankton biochronology for the last 772,000 years

The bioevents recorded in GL-852 correlate well with those exhibited in core GL-854 through the studied interval. Our results show little differences in the chronostratigraphic position of some bioevents in both calcareous nannofossil and planktonic foraminifera groups when compared to those ages in the literature data, although no clear pattern was observed. As pointed out by Raffi (2002) we also believe these differences may reflect the influence of regional environmental conditions on diachronous placement of biological datum events. In this sense, our results show that planktonic foraminifera events have been more diachronic than the calcareous nannofossils events.

Before 480 ka (MIS 13) the events related to the cyclic appearances and disappearances of the *G. menardii* complex occurred first in Santos Basin and later in the Gulf of Mexico. After 480 ka, these events in the

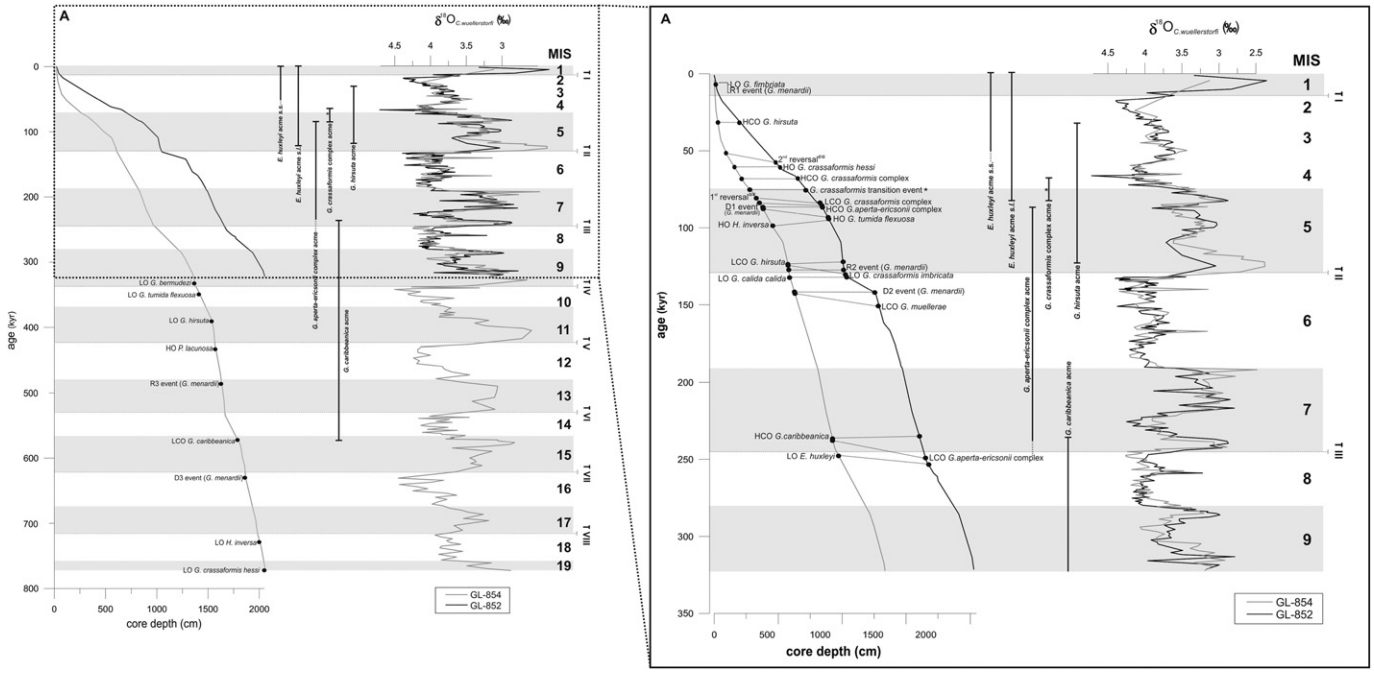

Fig. 6. Summary of the positions of the biohorizons since 772 ka and their relationship with the oxygen isotope curve. Gray bands correspond to marine isotope stages, identified by numbers on the right. Horizontal dotted lines indicate glacial terminations (T VIII to T I). LO, lowest occurrence; HO, highest occurrence; LCO, lowest common occurrence; HCO, highest common occurrence; D, *G. menardii* complex virtual disappearances; R, *G. menardii* complex virtual reappearances; T, Termination.

South Atlantic have always occurred after those observed in the Gulf of Mexico. On the other hand, the bioevents of both calcareous nannofossils and planktonic foraminifera seem to have occurred earlier in the Pacific than in South Atlantic Ocean. For calcareous nannofossils, the events observed in this study were recorded earlier in the Southern Ocean and Cape Basin and later in the North Atlantic. Our samples recorded an intermediate age, which is expected since the study area is located between the Southern Ocean and the North Atlantic. An exception was noticed for the LO of *E. huxleyi*, which was first recorded in the North Atlantic and later in the western South Atlantic Ocean. These age differences were calculated between 12 and 15 kyr. This event seems to have a similar behavior to that reported by Hine and Weaver (1998) for the eastern North Atlantic Ocean: a slightly time-transgressive event occurring in progressively younger sediments from north to south. To some extent, this assertion may have a wider application than only the eastern North Atlantic since the oldest records of LO *E. huxleyi* are from the northernmost Atlantic Ocean (Hine, 1990 in Hine and Weaver, 1998) and the younger ones are in the South Atlantic. It may suggest a migration of this species from north to south during its evolution in the Atlantic Ocean.

Comparing our biostratigraphic framework to that of Sato et al. (2009), which also correlates the nannofossil datum events with oxygen isotope stratigraphy. They placed the datum of the LO of *E. huxleyi* and the HO of *P. lacunosa* in MIS 8 and MIS 12 respectively, just before the highest peak of each respective MIS. Sato et al. (2009) have argued their high resolution study has clarified the critical stratigraphic positions of both datums. Although the stratigraphic position of LO *E. huxleyi* and HO *P. lacunosa* are correlated to the final portion of MIS 8 and MIS12, respectively, in our study their positions are traced to the highest peak of MIS 8 and MIS 12 (Fig. 6), which slightly differs from the North Atlantic datums. Fig. 6 also shows roughly a succession of both planktonic foraminifera and calcareous nannofossil events as well as a sequence of six superimposed "acmes" since the end of MIS 15.

The oldest acme recorded in this study was the *G. caribbeanica* acme, from MIS 15 until the MIS 7e-7d transition followed by the *G. aperta* + *G. ericsonii* complex acme, which intersects *G. caribbeanica* acme at the MIS 7e peak. This acme extended until the MIS 5c-5b transition. Just before, at the MIS 5e-5d transition begins the *G. hirsuta* acme, which extend up to MIS 3 near to MIS 3/MIS 2 transition. In the middle of the *G. hirsuta* acme the *G. crassaformis* complex acme (LCO to HCO of *G. crassaformis* complex) is easily recognized. In our record, this acme was traceable from MIS 5b to MIS 4. During the *G. crassaformis* complex acme, we noticed what we called *E. huxleyi* acme s.l. (from the first increase in *E. huxleyi* abundance) from MIS 5a to recent. Lately, still within *G. hirsuta* acme, we recognized the *E. huxleyi* acme s.s. (from when *E. huxleyi* dominance is indubitable) very close to the highest peak of MIS 3.

The bioevents identified in this study have been observed in almost all marine isotopic stages except MIS 2, 14 and 17. The calcareous nannofossil evolutionary events are related to glacial stages: LO of *H. inversa* (MIS 18), HO of *P. lacunosa* (MIS 12) and LO of *E. huxleyi* (MIS 8) with the exception of HO of *H. inversa* that occurs in the interglacial MIS 5, although during the cold substage 5d. On the other hand, those events related to abundance variation were found during interglacial stages: LCO of *G. caribbeanica* (MIS 15), HCO of *G. caribbeanica* (MIS 7), LCO of the *G. aperta-ericsonii* complex (MIS 7), HCO of the *G. aperta-ericsonii* complex (MIS 5) and the first reversal between small *Gephyrocapsa*/*E. huxleyi* (MIS 5). Except for the LCO of *G. muellerae*, which occurs during the glacial MIS 6.

In contrast, the planktonic foraminifera evolutionary events were mostly recorded during interglacials. This is the case of the LO of *G. crassaformis hessi* (MIS 19), LO of *G. hirsuta* (MIS 11), LO of *G. bermudezi* (MIS 9), LO of *G. crassaformis imbricata* (MIS 5), HO of *G. tumida flexuosa* (MIS 5) and LO of *G. fimbriata* (MIS 1). However, only three events occurred during glacials: LO of *G. tumida flexuosa* (MIS 10), LO of *G. calida calida* (MIS 6) and HO of *G. crassaformis hessi* (MIS 4). The species abundance events of planktonic foraminifera were also recorded during interglacials: LCO of *G. hirsuta* (MIS 5), LCO of *G. crassaformis* complex (MIS 5) and all reappearance events of the *G. menardii* complex (MIS 13, 5 and 1). Those bioevents related to decreasing abundance were recorded during glacials: HCO of the *G. crassaformis* complex (MIS 4), HCO of *G. hirsuta* (MIS 3) and the disappearance events of the *G. menardii* complex (MIS 16, and MIS 6). The exception was D1 event, the last disappearance event of the *G. menardii* complex, which occurs in the interglacial MIS 5, although during the cold substage 5b.

5. Conclusions

The cores selected for this study are located in a key region and provide an opportunity to study the evolution of calcareous nannofossil and planktonic foraminifera assemblages in the South Atlantic. We constructed a biostratigraphic framework that can be useful for tropical regions of the Atlantic, and provides high-resolution quantitative records of the most important species of coccolithophorids and foraminifers for a large part of the Pleistocene. Twelve Pleistocene calcareous nannofossil events and twenty planktonic foraminifera events calibrated with the oxygen isotope record and correlated with literature stratigraphies are discussed. This is the first calcareous plankton biochronology study for the last 772 kyr in the western South Atlantic Ocean. Calcareous nannofossil events show minimum diachronism with respect to the same events identified in different locations. On the other hand, planktonic foraminifera events are more diachronous according to the literature. Further studies in this region will help to establish a more precise biochronology for these calcareous microfossils. This study also presented six new biostratigraphic events of planktonic foraminifera isotopically calibrated. These bioevents can be used as markers in the western South Atlantic: LO of *G. bermudezi,* LCO of *G. hirsuta*, HCO of *G. hirsuta*, LCO of the *G. crassaformis* complex, HCO of the *G. crassaformis* complex and the *G. crassaformis* transition event (MIS 5/MIS 4).

Acknowledgements

This study is a contribution of the Applied Micropaleontology Program, funded by Petrobras, by São Paulo Research Foundation (FAPESP) grant 2013/50224-2 and by the bilateral collaborative research council for international research between Salamanca University (Spain) and University of São Paulo (Brazil) grant 2011-9 and the project VCACLIODP339 (CTM2012-38248) from the Spanish Ministerio de Economía y Competitividad. The authors wish to express their thanks to Petrobras for providing the samples. We are especially grateful to Renato Kowsmann for useful discussions and for emphasizing the need to properly integrate the biostratigraphic and isotopic data for Santos Basin. The authors are also thankful to the Laboratório de Paleoceanografia do Atlântico Sul – (LaPAS-IOUSP) staff for sample preparation and technical support. This manuscript greatly benefitted from the contributions of two anonymous reviewers.

Appendix A. Supplementary data

Supplementary data to this article can be found online at http://dx.doi.org/10.1016/j.marmicro.2016.07.002.

References

Aksu, A.E., Kaminski, M.A., 1989. Neogene planktonic foraminiferal biostratigraphy and biochronology in Baffin Bay and the Labrador Sea. In: Srivastava, S.P., Arthur, M., Clement, B., et al. (Eds.), Proc. ODP, Scientific Results, 105: College Station, TX (Ocean Drilling Program), pp. 287–304 http://dx.doi.org/10.2973/odp.proc.ir.105.1987.

Antunes, R.L., 1994. Bioestratigrafia dos Nanofósseis Quaternários da Bacia de Campos. Bol. Geosci. Petrobras 8 (2/4), 295–313.

Antunes, R.L., 1997. Introdução ao estudo dos nanofósseis calcários. UFRJ, Rio de Janeiro (115 pp.).

Antunes, R.L., 2007. Nanofósseis calcários do Quaternário da margem continental brasileira. Rio de Janeiro, CENPES/PETROBRAS (76 p. (Série Ciência Técnica Petróleo 21)).

Berger, W.H., Wefer, G., 1996. Expeditions into the past: paleoceanographic studies in the South Atlantic. In: Wefer, G., Berger, W.H., Siedler, G., Webb, D.J. (Eds.), The South Atlantic: Present and Past Circulation. Springer-Verlag, pp. 363–410.

Berggren, W.A., Hilgen, F.J., Langereis, C.C., Kent, D.V., Obradovich, J.D., Raffi, I., Raymo, M., Shackleton, N.J., 1995. Late neogene chronology: new perspectives in high-resolution stratigraphy. Geol. Soc. Am. Bull. 107, 1272–1287.

Bolli, H.N., Premoli Silva, I., 1973. Oligocene to recent planktonic foraminifera and stratigraphy of the Leg 15 sites in the Caribbean Sea. Initial Rep. Deep Sea Drill. Proj. 15, 475–497.

Bolli, H.M., Saunders, J.B., 1985. Oligocene to Holocene low latitude planktic foraminifera. In: Bolli, H.M., Saunders, J.B., Perch-Nielsen, K. (Eds.), Plankton Stratigraphy. Cambridge Earth Science Series vol. 1. Cambridge University, Cambridge, pp. 155–262.

Bollmann, J., Baumann, K.-H., Thierstein, H.R., 1998. Global dominance of *Gephyrocapsa* coccoliths in the late Pleistocene: selective dissolution, evolution, or global environmental change? Paleoceanography 13 (5), 517–529.

Bown, P.R., 1998. Calcareous Nannofossil Biostratigraphy. Kluwer Academic Publishers (314pp.).

Broecker, W., Pena, L.D., 2014. Delayed Holocene reappearance of *G. menardii*. Paleoceanography 29, 291–295. http://dx.doi.org/10.1002/2013PA002590.

Butzin, M., Prange, M., Lohmann, G., 2005. Radiocarbon simulations for the glacial ocean: the effects of wind stress, Southern Ocean sea ice and Heinrich events. Earth Planet. Sci. Lett. 235, 45–61.

Bylinskaya, M.E., 2005. Range and stratigraphic significance of the *Globorotalia crassaformis* plexus. J. Iber. Geol. 31 (1), 51–63.

Caley, T., Giraudeau, J., Malaizé, B., Rossignol, L., Pierre, C., 2012. Agulhas leakage as a key process in the modes of quaternary climate changes. Proc. Natl. Acad. Sci. U. S. A. 109 (18), 6835–6839. http://dx.doi.org/10.1073/pnas.1115545109.

Camillo, J.R.,.E., 2007. Foraminíferos planctônicos Em Resposta às mudanças oceanográficas no Atlântico Tropical oeste durante os últimos 30.000 anos. Dissertação de Mestrado, Instituto Oceanográfico da Universidade de São Paulo (206 p).

Camillo, J.R.,.E., Quadros, J.P., Costa, K.B., Toledo, F.A.L., 2015. Análises faunística e multivariada de foraminíferos planctônicos da Bacia Pernambuco-Paraíba: uma interpretação paleoambiental dos últimos 30 mil anos. Rev. Bras. Paleontol. 18 (1), 109–120.

Chang, H.K., Kowsmann, R.O., 1987. Interpretação genética das seqüências estratigráficas das Bacias da Margem Continental Brasileira. Rev. Bras. Geosci. 17 (2), 74–80.

Chang, H.K., Kowsmann, R.O., Figueiredo, A.M.F., Bender, A., 1992. Tectonics and stratigraphy of the East Brazil rift system. Tectonophysics 213, 97–138.

Chaproniere, G.C.H., Styzen, M.J., Sager, W.W., Nishi, H., Quinterno, P.J., Abrahamsen, N., 1994. Late Neogene biostratigraphic and magnetostratigraphic synthesis, Leg 135. In: Hawkins, J., Parson, L., Allan, J., et al. (Eds.), Proceedings of the Ocean Drilling Program, Scientific Results, College Station, TX (Ocean Drilling Program) 135, pp. 857–877. http://dx.doi.org/10.2973/odp.proc.sr.135.116.1994.

Cobbold, P.R., Meisling, K.E., Mount, V.S., 2001. Reactivation of an obliquely rifted margin, Campos and Santos basins, southeastern Brazil. AAPG Bull. 85, 1925–1944.

de Almeida, F.K., de Mello, R.M., Costa, K.B., Toledo, F.A.L., 2015. The response of deep-water benthic foraminiferal assemblages to changes in paleoproductivity during the Pleistocene (last 769.2 kyr), western South Atlantic Ocean. Palaeogeogr. Palaeoclimatol. Palaeoecol. 440, 201–212.

Demercian, S., Szatmari, P., Cobbold, P.R., 1993. Style and pattern of salt diapirs due to thin-skinned gravitational gliding, Campos and Santos basins, offshore Brazil. Tectonophysics 228, 393–433.

Duarte, C.S.L., Viana, A.R., 2007. Santos Drift System: stratigraphic organization and implications for the late Cenozoic palaeocirculation in the Santos Basin, SW Atlantic Ocean. In: Viana, A.R.; Rebesco, M. (Eds.). Economic and palaeoceanographic significance of contourite deposits. Geol. Soc. Lond., Spec. Publ. 276, 171–198.

Ericson, D.B., Wollin, G., 1968. Pleistocene climates and chronology in deep-sea sediments. Science 162, 1227–1234.

Fairbanks, R.G., Mortlock, R.A., Chiu, T.-C., Cao, L., Kaplan, A., Guilderson, T.P., Fairbanks, T.W., Bloom, A.L., 2005. Marine radiocarbon calibration curve spanning 10,000 to 50,000 years B.P. based on paired $^{230}Th/^{234}U/^{238}U$ and ^{14}C dates on pristine corals. Quat. Sci. Rev. 24, 1781–1796.

Ferreira, F., Leipnitz, I.I., Vicalvi, M.A., Sanjinés, A.E.S., 2012. Zoneamento Paleoclimático do Quaternário da Bacia de Santos com base em foraminíferos planctônicos. Rev. Bras. Paleontol. 15 (2), 173–188.

Flores, J.-A., Gersonde, R., Sierro, F.J., 1999. Pleistocene fluctuations in the Agulhas current retroflection based on the calcareous plankton record. Mar. Micropaleontol. 37, 1–22.

Flores, J.-A., Gersonde, R., Sierro, F.J., Niebler, H.S., 2000. Southern Ocean Pleistocene calcareous nannofossil events: calibration with isotope and geomagnetic stratigraphies. Mar. Micropaleontol. 40, 377–402.

Flores, J.-A., Marino, M., 2002. Pleistocene calcareous nannofossil stratigraphy for ODP leg 177 (Atlantic sector of Southern Ocean). Mar. Micropaleontol. 45, 191–224.

Flores, J.-A., Marino, M., Sierro, F.J., Hodell, D.A., Charles, C.D., 2003. Calcareous plankton dissolution pattern and coccolithophore assemblages during the last 600 kyr at ODP site 1089 (Cape Basin, South Atlantic): paleoceanographic implications. Palaeogeogr. Palaeoclimatol. Palaeoecol. 196, 409–426.

Gartner, S., 1977. Calcareous nannofossil biostratigraphy and revised zonation of the Pleistocene. Mar. Micropaleontol. 2, 1–25.

Golovina, L.A., Bylinskaya, M.E., Vernigorova, Y.V., 2008. Middle Pleistocene–Holocene calcareous plankton and benthos biostratigraphy of the Markova depression, equatorial Atlantic. Stratigr. Geol. Correl. 16 (3), 317–327.

Hemleben, C., Spindler, M., Anderson, O.R., 1989. Modern Planktonic Foraminifera. Springer, Berlin, Heidelberg, New York (363 pp.).

Hine, N., Weaver, P.P.E., 1998. Quaternary. In: Bown, P.R. (Ed.), Calcareous Nannofossil Biostratigraphy. Chapman; Hall, London, pp. 266–283.

Hine, N., 1990. Late Cenozoic Calcareous Nannoplankton from the Northeast Atlantic (Ph.D. Thesis) University of East Anglia.

Jordan, R.W., Zhao, M., Eglinton, G., Weaver, P.P.E., 1996. Coccolith and alkenone stratigraphy at a NW Africa upwelling site (ODP 658C) over the last 130,000 years. In: Moguilevsky, A., Whatley, R. (Eds.), Microfossils and Oceanic Environments. University of Wales Aberystwyth Press, pp. 111–130.

Jorissen, F.J., Asioli, A., Borsetti, A.M., Capotondi, L., de Vischer, J.P., Hilgen, F.J., Van der Borg, K., Vergnaud-Grazzini, C., Zachariasse, W.J., 1993. Late Quaternary central Mediterranean biochronology. Mar. Micropaleontol. 21, 169–189.

Kohl, B., Fillon, R.H., Roberts, H.H., 2004. Foraminiferal biostratigraphy and paleoenvironments of the Pleistocene Lagniappe delta and related section, northeastern Gulf of Mexico. In: Andersen, J.B., FILLON, R. (Eds.), Late Quaternary Stratigraphic Evolution of the Gulf of Mexico Basin. SEPM Spec. Publ. 79, pp. 189–216.

Lisiecki, L.E., Raymo, M.E., 2005. A Pliocene-Pleistocene stack of 57 globally distributed benthic $\delta^{18}O$ records. Paleoceanography 20.

Macedo, J.M., 1989. Evolução tectônica da Bacia de Santos e áreas continentais adjacentes. Bol. Geosci. Petrobras 3 (3), 159–173.

Macedo, J.M., 1990. Evolução tectônica da Bacia de Santos e áreas continentais adjacentes. In: Raja Gabaglia, G.P., Milani, E.J. (Eds.), Origem e evolução de bacias sedimentares. PETROBRAS, Rio de Janeiro, pp. 361–376.

Maciel, D.M., Alves, C.F., Ferreira, E.P., 2012. Bioestratigrafia com base em Nanofósseis Calcários do testemunho GL-77, Bacia de Campos, Sudeste do Brasil. Rev. Bras. Paleontol. 15 (2), 164–172.

Maiorano, P., Tarantino, F., Marino, M., Girone, A., 2013. A paleoecological and paleobiogeographic evaluation of *Helicosphaera inversa* (Gartner) Theodoridis and the diachrony of its first occurrence. Mar. Micropaleontol. 104, 14–24. http://dx.doi.org/10.1016/j.marmicro.2013.08.001.

Marino, M., Maiorano, M., Monechi, S., 2003. Quantitative Pleistocene calcareous nannofossil biostratigraphy of Leg 86 Site 577 (Shatsky Rise, Northwestern Pacific Ocean). J. Nannoplankton Res. 25 (1), 25–37.

Martin, R.E., Neff, E.D., Johnson, G.W., Krantz, D.E., 1990. Biostratigraphy of the Pleistocene: the Ericson and Wollin zonation revisited. Society of Economic Paleontologists and Mineralogists (Gulf Coast Section). Eleventh Annual Research Conference: "Sequence Stratigraphy as an Exploration Tool: Concepts and Practices in the Gulf Coast", Houston, TX, December 2–5, Program with Papers, pp. 229–236.

Martin, R.E., Neff, E.D., Johnson, G.W., Krantz, D.E., 1993. Pleistocene sequence boundaries Gulf of Mexico. PALAIOS 8, 155–171.

Martinez, J.I., Mora, G., Barrows, T.T., 2007. Paleoceanographic conditions in the western Caribbean Sea for the last 560 kyr as inferred from planktonic foraminifera. Mar. Micropaleontol. 64, 177–188.

Martini, E., 1971. Standard tertiary and quaternary calcareous nannoplankton zonation. In: Farinacci, A. (Ed.)Proceedings of the Second Planktonic Conference Roma 1970 2, pp. 739–785.

Matsuoka, H., Okada, H., 1990. (1990) Time-progressive morphometric changes of the genus *Gephyrocapsa* in the quaternary sequence of the tropical Indian Ocean, Site 709. In: Duncan, R.A., Backman, J., Peterson, L.C., et al. (Eds.), Proceedings of the ODP, Scientific Results Vol. 115. Ocean Drilling Program, College Station, TX, pp. 255–270.

Meisling, K.E., Cobbold, P.R., Mount, V.S., 2001. Segmentation of an obliquely-rifted margin, Campos and Santos basins, southeastern Brazil. AAPG Bull. 85 (11), 1903–1924.

Modica, C.J., Brush, E.R., 2004. Post rift sequence stratigraphy, paleogeography, and fill history of the deep-water Santos Basin, offshore southeast Brazil. AAPG Bull. 88, 923–946.

Mohriak, W.U., Macedo, J.M., Castellani, R.T., Rangel, H.D., Barros, A.Z.N., Latge, M.A.L., Mizusaki, A.M.P., Szatmari, P., Demercian, L.S., Rizzo, J.G., Aires, J.R., 1995. Salt tectonics and structural styles in the deep-water province of the Cabo Frio region, Rio de Janeiro, Brazil. In: Jackson, M.P.A., Roberts, D.G., Snelson, S. (Eds.), Salt Tectonics. A Global Perspective: AAPG Memoir Vol. 65, pp. 273–304.

Paillard, D., Labeyrie, L., Yiou, P., 1996. Macintosh program performs time-series analysis, EOS Trans. AGU 77, 379.

Patterson, R.T., Fishbein, E., 1989. Re-examination of the statistical methods used to determine the number of point counts needed for micropaleontological quantitative research. J. Paleontol. 63, 245–248.

Perch-Nielsen, K., 1989. Cenozoic calcareous nannofossils. In: Bolli, H.H., Saunders, J.B., Perch-Nielsen, K. (Eds.), Plankton Stratigraphy. Cambridge University Press, pp. 427–554.

Pereira, M.J., Macedo, J.M., 1990. A Bacia de Santos: perspectivas de uma nova província petrolífera na plataforma continental sudeste brasileira. Bol. Geosci. Petrobrás 4, 3–11.

Pereira, M.J., 1994. Seqüências deposicionais de 2ª/3ª ordens (50 a 2,0 Ma) e tectono-estratigrafia no Cretáceo de cinco bacias marginais do Brasil. Comparações com outras áreas do globo e implicações geodinâmicas. Tese de Doutorado, Instituto de Geociências, Universidade Federal Do Rio Grande Do Sul, Porto Alegre (271 p).

Pivel, M.A.G., Santarosa, A.C.A., Toledo, F.A.L., Costa, K.B., 2013. The Holocene onset in the southwestern South Atlantic. Palaeogeogr. Palaeoclimatol. Palaeoecol. 374, 164–172.

Portilho-Ramos, R.C., Rios-Netto, A.M., Barbosa, C.F., 2006. Caracterização bioestratigráfica do Neógeno superior da Bacia de Santos com base em foraminíferos planctônicos. Rev. Bras. Paleontol. 9, 349–354.

Portilho-Ramos, R.C., Barbosa, C.F., Rios-Netto, A.M., 2014. Planktonic foraminiferal variations in the southwestern Atlantic since the last glacial–interglacial cycle. PALAIOS 29, 38–44. http://dx.doi.org/10.2110/palo.2012.104.

Pujol, C., Duprat, J., 1983. Quaternary planktonic foraminifers of the southwestern Atlantic (Rio Grande Rise) Deep Sea Drilling Project Leg 72. In: Barker, P.F., Carlson, R.L., Johnson, D.A., et al. (Eds.), Initial Reports of the Deep Sea Drilling Project 72, pp. 601–615.

Pujos, A., Giraudeau, J., 1993. Répartition des Noelaerhabdaceae (nannofossiles calcaires) dans le Quaternaire moyen et supérieur des océans Atlantique et Pacifique. Oceanol. Acta 16, 349–362.

Raffi, I., Backman, J., Rio, D., Shackleton, N.J., 1993. Plio-Pleistocene nannofossil biostratigraphy and calibration to oxygen isotope stratigraphies from Deep Sea Drilling Project Site 607 and Ocean Drilling Program Site 677. Paleoceanography 8, 387–408.

Raffi, I., 2002. Revision of the early-middle pleistocene calcareous nannofossil biochronology (1.75–0.85 Ma). Mar. Micropaleontol. 45, 25–55.

Raffi, I., Backman, J., Fornaciari, E., Pälike, H., Rio, D., Lourens, L., Hilgen, F.J., 2006. A review of calcareous nannofossil astrobiochronology encompassing the past 25 million years. Quat. Sci. Rev. 25, 3113–3137.

Railsback, L.B., Gibbard, P.L., Head, M.J., Voarintsoa, N.R.G., Toucanne, S., 2015. An optimized scheme of lettered marine isotope substages for the last 1.0 million years, and the climatostratigraphic nature of isotope stages and substages. Quat. Sci. Rev. 111, 94–106.

Rodrigues, R., Rothstein, L.M., Wimbush, M., 2007. Seasonal variability of the south equatorial current bifurcation in the Atlantic Ocean: a numerical study. J. Phys. Oceanogr. 37, 16–30.

Sato, T., Chiyonobu, S., Hodell, D.A., 2009. Quaternary calcareous nannofossil datums and biochronology in the North Atlantic Ocean, IODP Site U1308. Proc. IODP vol. 303.

Sanjinés, A.E.S., 2006. Biocronoestratigrafia de foraminíferos em três testemunhos do Pleistoceno-Holoceno do talude continental Da Bacia de Campos, RJ – Brasil. Dissertação de Mestrado, Instituto de Geociências. Universidade Federal do Rio de Janeiro (119 pp.).

Sexton, P.F., Norris, R.D., 2011. High latitude regulation of low latitude thermocline ventilation and planktic foraminifer populations across glacial-interglacial cycles. Earth Planetary Science Letters 311, 69–81. http://dx.doi.org/10.1016/j.epsl.2011.08.044.

Stramma, L., England, M., 1999. On the water masses and mean circulation of the South Atlantic Ocean. J. Geophys. Res. 104 (C9), 20863–20883.

Takayama, T., Sato, T., 1987. Coccolith biostratigraphy of the North Atlantic Ocean, Deep Sea Drilling Project Leg 94. In: Ruddiman, W.E., Kidd, R.B., Thomas, E., et al. (Eds.), Init. Repts. DSDP 94 (Pt. 2). U.S. Govt. Printing Office, Washington, pp. 651–702.

Thierstein, H.R., Geitzenauer, K.R., Molfino, B., Shackleton, N.J., 1977. Global synchroneity of late quaternary coccolith datum levels: validation by oxygen isotopes. Geology 5, 400–404.

Tokutake, L.R., Toledo, F.A.L., 2007. Bioestratigrafia de Nanofósseis Calcários e Estratigrafia de Isótopos (C e O) do Talude médio, Quaternário, porção norte da Bacia de Campos, Brasil. In: Carvalho, I., Cassab, R., Schwanke, C., Carvalho, M., Fernandes, A., Rodrigues, M., Carvalho, M., Arai, M., Oliveira, M.E. (Eds.), Paleontologia: Cenários Da Vida. Rio de Janeiro: Interciência Ltda vol. 2, pp. 395–410.

Toledo, F.A.L., 2000. Variações Paleoceanográficas nos últimos 30.000 anos no oeste do Atlântico Sul: isótopos de oxigênio, assembleia de foraminíferos planctônicos e nanofósseis calcários (Tese de doutorado) Universidade Federal Do Rio Grande Do Sul, Porto Alegre, RS (245 p).

Vicalvi, M.A., 1997. Zoneamento bioestratigráfico e paleoclimático dos sedimentos do Quaternário Superior do Talude da Bacia de Campos. Bol. Geosci. Petrobrás 11 (1/2), 132–165.

Vicalvi, M.A., 1999. Zoneamento bioestratigráfico e paleoclimático do Quaternário Superior do talude da Bacia de Campos e Platô de São Paulo adjacente, com base em foraminíferos planctônicos (Tese de Doutorado) Universidade Federal do Rio de Janeiro, Rio de Janeiro, RJ (183 pp.).

Wade, B.S., Pearson, P.N., Berggren, W.A., Pälike, H., 2011. Review and revision of Cenozoic tropical planktonic foraminiferal biostratigraphy and calibration to the geomagnetic polarity and astronomical time scale. Earth-Sci. Rev. 104, 111–142.

Wefer, G., Berger, W.H., Bickert, T., Donner, B., Fischer, G., Kemle-von Mücke, S., Meinecke, G., Müller, P.J., Mulitza, S., Niebler, H.-S., Pätzold, J., Schmidt, H., Schneider, R.R., Segl, M., 1996. Late Quaternary surface circulation of the South Atlantic: the stable isotope record and implications for heat transport and productivity. In: Wefer, G., Berger, W.H., Siedler, G., Webb, D.J. (Eds.), The South Atlantic: Present and Past Circulation. Springer-Verlag, Berlin, pp. 461–502.

Wei, W., 1993. Calibration of upper Pliocene–lower Pleistocene nannofossil events with oxygen isotope stratigraphy. Paleoceanography 8 (1), 85–99. http://dx.doi.org/10.1029/92PA02504.